Review

A Comprehensive Review of Polymeric Wastewater Purification Membranes

Rasmeet Singh [1],*, Mandeep Singh [2], Nisha Kumari [3], Janak [3], Sthitapragyan Maharana [2] and Pragyansu Maharana [2]

1   Dr. S.S. Bhatnagar University Institute of Chemical Engineering & Technology, Panjab University, Chandigarh 160014, India
2   School of Mechanical and Mechatronic Engineering, University of Technology Sydney, 15 Broadway, Sydney, NSW 2007, Australia; Mandeep.Singh@uts.edu.au (M.S.); sthitapragyan.maharana@student.uts.edu.au (S.M.); pragyansu.maharana@student.uts.edu.au (P.M.)
3   Dr. B.R. Ambedkar National Institute of Technology Jalandhar, Jalandhar 144011, India; nishusharma231115@gmail.com (N.K.); jk199chauhan@gmail.com (J.)
*   Correspondence: srasmeet9@gmail.com

Abstract: Synthetic membranes are currently employed for multiple separation applications in various industries. They may have been prepared from organic or inorganic materials. Present research majorly focuses on polymeric (i.e., organic) membranes because they show better flexibility, pore formation mechanism, and thermal and chemical stability, and demand less area for installation. Dendritic, carbon nanotube, graphene and graphene oxide, metal and metal oxide, zwitter-ionic, and zeolite-based membranes are among the most promised water treatment membranes. This paper critically reviews the ongoing developments to utilize nanocomposite membranes to purify water. Various membranes have been reported to study their resistance and fouling properties. A special focus is given towards multiple ways in which these nanocomposite membranes can be employed. Therefore, this review provides a platform to develop the awareness of current research and motivate its readers to make further progress for utilizing nanocomposite membranes in water purification.

Keywords: carbon nanotubes; dendrimers; waste water purification; zeolites; zwitterion

1. Introduction

Water dearth and decontamination widely alter the sustainable development of global and societal activities. The crises of imbalance between both demand and supply of quality water is a growing concern of the 21st century [1]. Based on the continuously growing population and urbanization, the year 2050 is expected to face an increased water demand of 40%, leaving 1.8 billion of the population in water-deficient situations. In India, around 75% of households are short of clean drinking water, and by 2030, 40% of the total population will completely run out of drinking water. Considering water quality, an adequate fresh supply of clean water has become a pivotal challenge. At present, almost 80% of wastewater worldwide is released without any pre-treatment into our water bodies, causing various water-borne diseases. Particularly in India, around 200,000 people die every year because of the unavailability of clean drinking water [2]. Present-day infrastructure for wastewater treatment and safe water production struggles to keep pace with demand within both developed and developing nations. Therefore, the growth of economical and efficient water purification systems is urgently required.

The membrane is an interface between two different phases and works as a selective barrier. Mechanisms followed by separation membranes are highly motivated by the natural world. For example, the exchange of materials between stomachic tissues of the body and the liver is quite similar to microfiltration and ultrafiltration processes. Membrane technologies are becoming an important aspect of industrial effluent treatment, including

those in the pharmaceutical, food, biotechnology, petrochemical, and chemical industries. Membranes are also employed for water purification in households and small commercial sites. In comparison to conventional separation materials, membranes offer economical and efficient treatment. Membranes also require less energy and raw materials for their preparation [3]. In fact, the synthesis materials can also be found in nature and hence are economical. Polymers and ceramics are the most widely used membrane materials. Polymers have attracted more attention due to their excellent mechanical and chemical stability [4]. Among the investigated materials, polymeric membranes such as polyvinylidene fluoride (PVDF), polyacrylonitrile (PAN), polyvinyl chloride (PVC), polysulfone (PSf), polyethylene (PE), polyamide, polyether sulfone (PES), polyvinyl chloride (PVC), polypropylene (PP), and polyvinyl alcohol (PVA) are applied the most. It is further found that PES and polyimide polymeric membranes experience the highest mechanical strength and operating temperature.

Dendrimers are considered to be novel synthetic polymeric nanostructures with balanced structure and a distinctive 3-D configuration. Its functional groups are capable of showing intermolecular interactions with various functional moieties. They are superior because of their exceptional properties, which are absent in linear polymers. Poly-(amidoamine) dendrimers are most widely used as an adsorbent for water purification [5]. They are non-toxic, cost-effective, and can be prepared from easily available materials. A section of this article will focus on dendrimer based materials for the adsorption of heavy metals, organic and inorganic pollutants, and dyes. Their adsorption mechanisms, fillers, and the influence of doping materials is intensively reviewed.

Advanced nanomaterials are also well-investigated compounds for water and wastewater purification. Carbon nanotubes and graphene/graphene oxide composites have shown positive results. These materials have a graphite-like carbon structure and follow the principle of adsorption and restrict the flow of pollutants [6]. The cost of fabrication of carbon nanotubes (CNTs) and graphene nano-composites poses a few challenges for their commercialization; however, these materials are the most potential candidates for the future of water purification. The paper also discusses a few chemical modifications for improving membrane performance and neutralizing the water-borne bacteria.

Incorporating nanoparticles (NPs) into polymeric membranes is another way of improving membrane properties. Nano-sized metals and their oxides have shown interesting properties when incorporated into polymeric membranes. They have shown enhancements in the optical, electronic, catalytic, and magnetic properties of the membrane [7]. Metal NPs of alumina, zirconium, silver, magnesium, and copper can be employed in almost every polymeric membrane to get targeted characteristics. These groups are mostly ionic and or comprises a lone pair of electrons that show chelating and stability effects on modified material. The above-mentioned metal NPs will be critically discussed in the upcoming sections.

Zwitter-ionic polymers are potential antifouling materials as they are capable of forming a hydration shell through electrostatic interactions. These interactions are much stronger than hydrogen bonds and thus result in closely packed adsorbed water [8]. In the past few years, a wide range of research has been carried out to incorporate zwitterionic materials on the membrane surface. Hence, a brief perspective of the most famous approaches is focused on in the present article.

Thin-film nanocomposite (TFN) membranes were first investigated in 2007, with an aim of enhancing membrane separation capacity, selectivity, and permeability properties. By introducing a minute amount of zeolite into polyamide (PA), water permeability can be highly improved. Zeolites also offer preferential flow paths to water molecules between its super hydrophilic passages and mesoporous structure [9].

Hence, the paper lays out the different characteristics and potential applications of nanoparticle membranes for water desalination applications. An intensive review of already developed technologies is covered based on their interactivities between different contaminants and polymeric nanomaterials such as carbon nanotubes, graphene/graphene

oxide (GO), metal/metal oxide, zwitter-ionic, and zeolite-based. Finally, the article highlights the future outlook and challenges existing practices.

2. Dendritic Polymers

These are polymers with random hyper branches. These mainly include spherical macro-molecules and are assembled with cross-linking shell morphology and terminal clusters, ultimately giving a well-defined structure [10]. Dendrimers may be of different formations, namely cone, disc, sphere, and more, and they can be in the range of 2–20 nm in size. These structures can be fabricated through the reaction of multiple dendrons with multi-functional characteristics. To date, hundreds of dendrimers have been synthesized with different surface modifications and compositions. Dendrimers act as adsorbents in the removal of heavy metal ions and organic pollutants. The inner shell of dendrimers is hydrophobic in nature and thus eases the adsorption of organic pollutants, whereas the outer shell consists of amine and hydroxyl functional groups that can adsorb the heavy metals present in wastewater. Dendrimer based polymers have come out to be an effective adsorbent for the removal of radionuclide as well as organic solvents from wastewater [11]. With all such characteristics, dendrimer polymers are among the best options for water and wastewater purification.

2.1. Titanium Supported Dendrimers

Titanium dioxide (TiO_2) modified by PAMAM dendrimers with ethylene diamine cores (G4-OH) were utilized for the removal of Cr(III), Cu(II), and Ni(II) from wastewater [12]. The immobilization strategy is displayed in Figure 1.
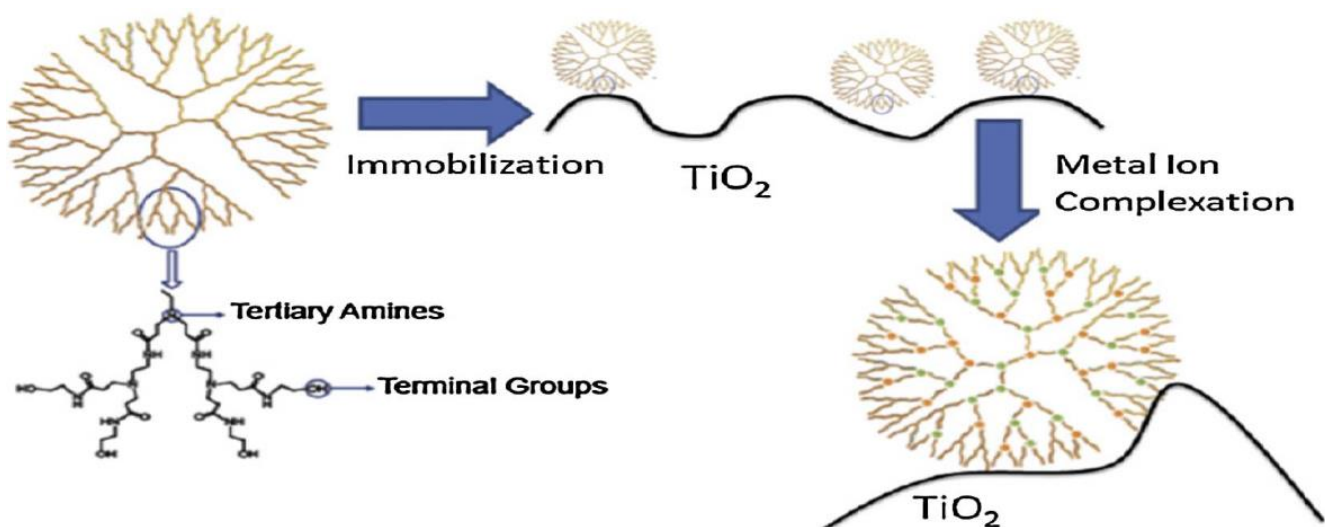

Figure 1. Strategy for immobilizing G4-OH dendrimers on titania to produce dendrimer/titania composites. Reprinted with permission from [12]. Copyright (2013) Elsevier Ltd.

The notable outcome regarding PAMAM modified TiO_2 was that the Brunauer–Emmett–Teller surface area of Ti remained similar to before. However, the removal rate and efficiency were improved with less operational time and a pH value of 7 and 9. The mixture also successfully removed Ni^{+2} ions better than the single system. Additionally, a PAMAM-Ti composite was employed for the removal of Pb(II) ions, which displayed the adsorption capacity of 400 mg/g [13]. Figure 2 suggests the removal mechanism of positive metal ions through dendrimers-Ti composite.
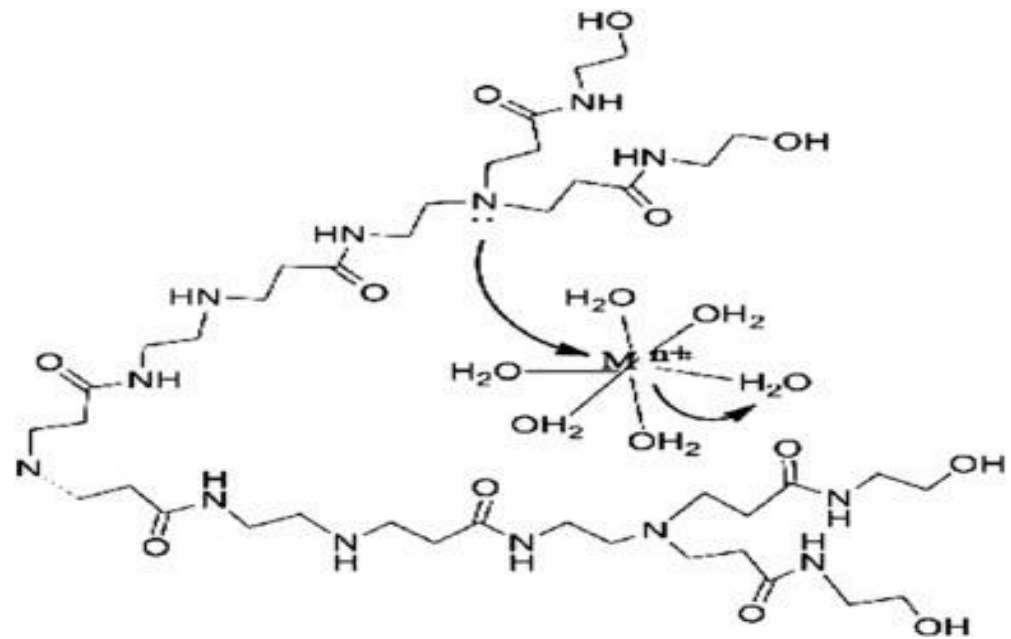
Figure 2. Mechanism for metal cations removal by PAMAM dendrimers–titania composites. Reprinted with permission from [12]. Copyright (2013) Elsevier Ltd.

Castillo et al. [14] studied the removal capacity of Ni and Fe oxidation states utilizing 4th generation PAMAM with the G4-OH group. They also investigated the influence of G4-OH immobilization on Ti enhanced materials and their chelating potential on Ni(II) removal. The results found that the potential of Ni(II) complexation towards idle PAMAM dendrimer gets inactive on Ti support. This behavior was explained mainly by two things; firstly, the limitations of diffusion in Ti pores, and secondly because of a decrease in the flexibility of PAMAM dendrimer, which leads to the increasing constraints for the accommodation of metal ions.

2.2. Magnetic Supports for Dendrimers

Separators utilizing magnetic particles offer finer phase separation and circumvent various steps of centrifugation and filtration in the post-removal cluster of adsorbents. Combining magnetic nanoparticles (MNPs) not only eases the adsorbent separation but also remarkably improves the adsorption capacity. It also limits the production of secondary waste from employed nanoparticles. In 2011, Chou et al. [15] investigated the elimination of Zn(II) from an aqueous mixture in a batch arrangement by utilizing G3-MNPs (i.e., dendrimer-conjugated magnetic nanoparticles) as adsorbents. As projected by the Langmuir model, the highest adsorption capacity came out to be 24.3 mg/g at 25 °C, with a pH of 7. Further, it was claimed that the removal capacity of Zn(II) was not much hindered, even after 10 consecutive cycles of adsorption and desorption.

Another research by Yen et al. [16] showed the formation of third-generation dendrimers on the surface of MNPs employed for the adsorption of metals such as Ag(I), Au(III), Pd(IV), and Pd(II). The adsorption value of greater valence metals such as Pd(IV) and Au(III) came out better than the lower value valence metals such as Pd(II) and Ag(I). Thus, it is concluded that the adsorption by precious metals on MNP-G3 varies in proportional to the valence value. Further, the regeneration was obtained by utilizing a 1% solution of hydrochloric acid.

PAMAM is also employed for the purposes of grafting dendrimers onto the surface of MNPs of silica. It was used for the decontamination of Hg(II) and MeHg(I). Both these ions are highly toxic in nature. Exposure to them can result in neurological and immunological disorders. The properties of PAMAM grafted with MNPs of silica (Fe_3O_4-SiO_2-PAMAMs) were enhanced through Coulomb attractions. Herring sperm type deoxyribonucleic acid

(DNA) fragments were immobilized onto a nanocomposite surface and hence acted as a reagent in mercury removal. Additionally, the Fe_3O_4–SiO_2 NPs get some traces of the hydroxyl group and itself becomes an adsorbent for Hg(II) and MeHg(I). The positive charge gets accumulated on the surface of NPs due to grafting. Additionally, increasing dendrimers result in a higher density of amines, leading to enhancement of net positive charge. In such conditions, the capacity of adsorbate decreases and Fe_3O_4-SiO_2 gets shielded with a negative hydroxyl group, thus leading to a coulombic force of repulsion to adsorbate. Hence, Hg(II) and MeHg(I) removal using Fe_3O_4-SiO_2-PAMAMs is poor. The efficiencies were thus increased through DNA immobilization onto the surface [17].

Kim el al. [18] have shown that the removal of heavy metals such as Pb(II) and Cd(II) is also effective through magnetic core dendrimers. The pH played an important role in the adsorption of heavy metals and regeneration of adsorbent. This is mainly due to the interactions between H^+ and metal ions. As the pH increases, the H^+ ions decrease, and hence the interactions also decreases. It is evident that higher pH results in effective adsorption, but at pH above 5, the lead and cadmium start to precipitate into hydroxides. Pb(II) has greater Pauling electronegativity and thus shows a high affinity towards sorbent and lone pair nitrogen in dendrimer amine groups. Furthermore, hydrochloric acid can be used as an extracting element to regenerate the adsorbent.

Pourjavadi et al. [19] synthesized PAMAM graft-poly (methyl acetate) dendrimer for the adsorption of lead ions from aqueous solution. It was produced first using radical of methyl acrylate polymerization. Then, PAMAM was used to functionalize the methyl ester group. The adsorbent displayed an adsorption capacity of 310 mg/g of lead ions. The adsorbent shows less activity at lower pH due to surface protonation. The preferred pH range is from 5 to 6, and above that, the lead ions precipitate into its hydroxide.

Zhou et al. [20] experimented the modified MNPs with PAMAM dendrimer for extraction of RBk5 (reactive black) from dye mixture. The results showed that the highest adsorption value of modified MNPs with the PAMAM dendrimer was 70.423 milligrams of RBk5 per gram of modified MNPs with PAMAM dendrimer. Additionally, the rate and kinetics of adsorption reduce with an increasing initial concentration of RBk5.

2.3. Dendrimers Supported on Nantural Materials

Natural materials are economical, abundant, environment friendly, and easily available. These have increased the interest for decontamination of wastewater pollutants in recent years. Chitin and cellulose are among the most easily available biopolymers. Chitin based cellulose and chitosan are widely preferred for bio-sorbent activities due to their non-toxicity, biocompatibility, and other outstanding adsorption properties. They are also employed for the removal of dyes and heavy metal ions [21]. Zhao el al. [22] showed a poly(amidoamine)-grafted cellulose nanofiber for the removal of Cr(VI) from aqueous solution. The bio-adsorbent displayed a low density and high porosity, while it was multi-functioning with an amine group. Further, its characterization disclosed that it has an open-cell-like geometry with sheet-like walls of interconnected cells. The pores were between 3 and 5 mm in size. Multiple peripheral pores of sizes 50–200 nm were also visible on each wall. The maximum removal capacity came out to be 377.36 mg/g, and this is the maximum reported capacity so far.

Chitosan is a nitrogen-containing polysaccharide, which is produced through the deacetylation of chitin. It is mostly found in terrestrial invertebrates, marine invertebrates, and lower forms of plants. Amine groups present in chitosan can be easily functionalized to Chitosan/poly(amidoamine) dendrimers for the efficient removal of dyes and heavy metal ions. Chitosan micro-particles can also be transformed into magnetic micro-particles, operationalized with polyamidoamine (PAMAM) dendrimers [21,23].

The good biocompatibility of an adsorbent is judged from its biocompatibility, surface area, hydrophilicity, and resistivity to chemicals and solvents. To enhance these properties, a cellulose membrane was implanted with Diaminobutane-poly (propyleneimine) functionalized with 16 thiol active group (DAB-3-$(SH)_{16}$) for the removal of heavy metals of a

toxic nature. Further, the membranes were characterized by electrochemical impedance spectroscopy (EIS) [24]. The bode plots reveal the decreasing Z_{real}, indicating heavy metal entrapment in the membrane, which results in an increasing number of charges.

2.4. Carbon-Based Supports for Dendrimers

Graphene oxide exhibits an oxidized functional branch and has a high surface area, due to which it acts as an excellent adsorbent for the removal of organic and inorganic pollutants. Yuan et al. [25] synthesized GO-PAMAMs by the grafting-form method for the adsorption applications of heavy metals. GO-PAMAMs, obtained through the grafting-form method, displayed higher adsorption capacity than GO. This was mainly due to the additional complexations among PAMAM amines and heavy metals. Similarly, Zhang et al. [26] obtained GO-PAMAMs through the grafting-to method and claimed that grafting-from is a superior method for synthesizing GO-PAMAMs.

Selenium (Se) falls under the category of trace nutrition. However, it can be highly toxic and harmful if ingested in excess. The toxicity levels of selenite and selenate are quite high. The elimination of Se(VI) is more difficult compared to Se(IV). Xiao et al. [27] synthesized GO-dendrimer, and the materials showed good removal capacity against selenium. It was facilitated mainly due to the high surface area of GO and the presence of multiple functional groups. The GO-PAMAM dendrimers acted as adsorbents for the Se(IV) and Se(VI) ions. The fraction of Se in the supernatant was measured after 24 h using inductively coupled plasma mass spectrometry (i.e., ICP-MS). The maximum adsorption results were shown by GO-G3 and GO-G4 adsorbents for Se(IV) and Se(VI), respectively. Further, it was noted that the adsorption of Se(VI) ions relies more upon the presence of the amine group. Because the interactions of selenite and selenate with GO-G4 are totally electrostatic, it mainly changes with initial pH values. At high pH, the primary and tertiary amine group gets deprotonated, and at lower pH values, the amine groups are protonated, and it also ensures more active binding sites for negative Se ions. GO-G4 displayed more adsorption capacity in comparison to both magnetic GO and pristine GO. At pH value 6, Se(IV) and Se(VI) showed adsorption capacities of 60.9 and 77.9 mg/g, respectively.

Iannazzo et al. [28] developed dendrimer on the surface of multiwall carbon nanotubes (MWCNTs) using triazole for the adsorption of heavy metals. The Moedritzer–Irani route was chosen for the synthesis of alpha-amino phosphonate nanosystem (MWCNT-TD$_2$P) amine group. The synthesized material displayed good chelating towards Pb(II), Hg(II), and Ni(II). Apart from this, the PAMAM-CNT nanocomposite exhibited high adsorption capacities of 4870 mg/g and 3333 mg/g towards Pb(II) and Cu(II), respectively [29].

2.5. Miscellaneous Dendrimers

Xu et al. [30] highlighted the applications of five major dendrimers, namely G1.0-NH$_2$, G1.5-COOH, G4.0-OH, G4.0-NH$_2$, and G4.5-COOH, where G is the generation number. A fixed bed column was utilized for experimental purposes. G4.5-COOH initially retained almost 90% of the copper at pH 6. Further, 100 mL of 2 normal (N) hydrochloric acid was used for the regeneration of dendrimer.

Gajjar et al. [31] produced triazine dendrimer with a hydroxyl terminal using the divergent method. No supporting material was used during the synthesis. The triazine dendrimer group that was synthesized included G0, G0.5, G1.0, G1.5, G2.0, G2.5, and G3.0. Out of these, half of the dendrimers appeared white in color and were insoluble in water due to chlorine termination. In comparison, the dendrimers with the hydroxyl terminal were brown in color and were very well water-soluble. The key result of the experiment was that the capacity of adsorption of these groups towards Cu, Ni, and Zn increases in direct proportion to the generation number.

PAMAM dendrimers were also employed in a fixed bed column to adsorb lead from contaminated soil. For regeneration of dendrimer, 2 N HCl, along with 94% dendrimer bounded PB^{2+} species, were extracted from dendrimers during acid regeneration [32]. Another study reported the synthesis of poly (methacrylic acid-g-PAMAM dendrimer)

using multiple proportions of nickel salt by gamma radiation-induced copolymerization of PAMAM dendrimer and methacrylic acid (MAA). Batch experiments were performed to study the adsorption effectivity of Cr(III), Cu(II), and Co(II) ions. Further, it was stated that nickel effectively enhanced the adsorption capacity of dendrimers towards Co(II) and Cu(II) ions. However, due to the different structural properties of Cr(III) and nickel, the dendrimer showed a decrease in adsorption capacity for the adsorption of Cr(III). Finally, a capacity of 16.37 mg/g, 17.2 mg/g, and 9.7 mg/g was obtained for Cr(III), Co(II), and Cu(II), respectively in the presence of 25 mg of Ni(II) at a pH value of 6 [33].

Beraa et al. [34] used 1st and 2nd generation phosphorous cationic dendrimers and sodium saturated montmorillonite for the adsorption of Cr(VI). Leather industries usually use Cr(VI) salts for surface treatment processes, and the effluents from these industries are usually filled with Cr(VI). The experimental analysis showed that GC2-montmorillonite, Na-montmorillonite, and GC1-montmorillonite can remove 7.15 mg/g, 6.2 mg/g, and 10.2 mg/g, respectively, of Cr(VI).

2.6. Outlook

Dendritic polymers are getting highlighted in various applications due to their adaptable structure and properties. In addition to exterior surface area, they offer high inside surface area to encapsulate targeted pollutants. As it can be comprehended from literature, dendrimers have not been substantially investigated in the field of removal. The common reason for this may be the requirement of expertise for its multistep synthesis. This can be overcome through research collaborations between different fields. Such practice can enable the designing of more cost-effective, selective, and target-oriented dendritic polymers. Along with focusing on one dendritic structure, it is very important to simultaneously investigate other dendritic polymers too. Novel and newly developed dendritic polymers must be benchmarked and compared with already existing adsorbents. Also, the already developed dendrimers should be modified in terms of removal efficiency, toxicity, mechanical and chemical strength and other important factors to improve the research environment. In conclusion, dendrimers have a very bright scope in removal applications and other different directions.

3. Carbon-Based Polymeric Membranes

Carbonaceous nanomaterials have high sorption capacity, selectivity, and surface area, due to which they act as potential sorbents to organic solutes in an aqueous medium. Along with this, they also exhibit good thermal conductivity, electrical conductivity, steady reactivity, and exceptional antioxidants. Highly discussed carbon nanomaterials include nanowires, activated carbon, carbon nanotubes (CNTs), diamonds, and fullerenes (C60) [35]. Genz et al. [36] utilized acids to enhance the colloidal stability of CNTs to remove Cr(VI). Multi-walled carbon nanotubes (MWCNTs) have proven their effectiveness in the adsorption of binary pollutants such as 2,4,6-trichlorophenol and Copper(II) ions. Additionally, chitosan nanoparticles display good absorption capabilities in the removal of acid dyes [37].

3.1. Carbon Nanotubes-Based Membranes

Carbon nanotubes are potential candidates for employing into wastewater treatment and purification. The pore size in nanometers can be altered by inner cores. Additionally, modifications in the growth process can be utilized to control the size of nanotubes. Hinds et al. [38] synthesized controlled nano-porous membranes through chemical-vapor deposition methods utilizing CNTs. The nanotubes obtained were in the range of 5–10 μm. Process simulations are an important part of examining water transportation through CNTs. Hummer et al. [39] demonstrated the chain transportation and permeation of water molecules in CNT without any friction. This happens because of the hydrogen bond formed between the water molecule and the inner core of CNT. Thomas and McGaughey [40] conducted the examination of dynamics of water directed by pressure in CNTs by varying the dimensions (i.e., diameter and length) of the tube. They also proposed a method to

configure the flow of water in CNTs and its dependence on tube diameter. It was noted that a single string chain of water molecules, having high flow velocity with fixed pressure, is accomplished in tube diameters of 0.83 nm.

CNTs are also very well known for rejecting dissolved ions during water desalination. The diameter of CNTs plays an important role in the selective exclusion of species [40]. One example of this has been demonstrated recently by K. Chen et al. [41]. He concluded that when the diameter of CNT is increased from 0.66 nm to 0.93 nm, the ion rejection efficiently decreases from 100% to 95%. Different studies have further revealed that 0.34 nm and 0.39 nm are the ideal diameters of CNTs for the rejection of sodium and chlorine ions, respectively [42]. However, it is quite difficult to achieve the swift flow of water molecules from an extremely small diameter CNTs. Instead, there are few effects observed on water flux and design elements to gain the optimal ion rejection at 0.6 nm to 0.8 nm diameter. Narrow tubes display less flux and also pose challenges in industrial-scale operations, such as reverse osmosis. Therefore, researchers are finding different ways in which CNTs with large diameters can be used for effective ion rejection applications. A few functional groups have also been suggested to improve the ion rejection capacity of CNTs. One of the mainly employed functional group is a carboxylate or amine group around the tip of CNT of diameter 10.9 nm. This addition blocks the entry of charged ion and improves the ion rejection capacity. However, this addition will reduce the water flux of the membrane [43]. Various important innovations in wastewater pollutants degradation using CNTs is given in Table S1 of supplementary file.

3.2. Graphene and Graphene Oxide-Based Membranes

Several methods, such as ball milling, electrochemical exfoliation, and high shear, have been suggested to synthesize graphene at affordable prices. Wang et al. [44] synthesized graphene through a new method called the pyridine-thermal exfoliation method. This methods uses pyridine as an intercalating dispersant and produces graphene with well capacitive deionization capacity. GO has a graphene lamellar structure with 1–30 μm thickness at the planes and edges. It has rich oxygen in the form of carboxyl and hydroxyl groups [45]. The presence of these oxygen groups signifies that graphite oxide has a complex structure. This also signifies that GO does not require any dispersant or stabilizer to stably disperse in water. This property turns out to be an extremely useful one during the process [46]. The oxygen-containing functional groups being susceptible to chemical reactions can be used for modifying GO chemically [47]. During the earl research into graphene, Brodie continuously treated graphite with potassium chlorite ($KClO_3$) and nitric acid (HNO_3) to obtain GO. Staudenmaier broadened the oxidation process through the utilization of sulfuric acid (H_2SO_4), $KClO_3$, and HNO_3. Hummer's method is the most widely used method for the synthesis of GO. It is a quick and secure process. Graphite powder can be extracted from brown oxidation graphite and high shear/ultrasonic intense agitation stripping [35]. This method has been regularly refined by adjusting oxidant quantity and time of oxidation, enabling the production of lamellar structures with different sizes. Alternative techniques such as liquid auxiliary electronic stripping [48], potassium ferrate [49], sealed oxidation [50], etc. have been investigated for improved oxidation of GO in terms of safety, environmental damage, and speed.

A few other methods used to prepare GO-based separation membranes include electric field induced-assembly, coating, layer-on-layer self-assembly, filtration, and evaporation. Filtration involves the dispersion of GO over a porous membrane (either a micro-filtration (MF) or ultra-filtration (UF) membrane) used as a substrate [51,52], either in vacuum or under pressure [53]. This further undergoes filtration, drying, and other processes, resulting in the formation of a porous membrane layer. Han et al. [54] synthesized a MWNT-intercalated nano-filtration membrane of graphene (G-CNTm). The graphene and CNT grains, which were dispersed and reduced, underwent filtration in a vacuum atmosphere within a PVDF UF membrane of 100 mm effective diameter to produce G-CNTm. This method may also be used for preparing GO films, ranging from several

nanometers to microns. However, the adjoining layers showed a fragile interface, hence the stability was less. The coatings can be applied to improve the membrane quality. This may be spin, cloth, or spray coating.

The demand for self-assembling GO nano-sheets is high. Sun et al. [55] prepared a new type of nano-filtration (NF)-membrane composite with PAN-UF membrane and coated it with a thin ethanol gel layer. Further, he prepared the GO film through the evaporation method. It was performed at an interface linking liquid and gas. The thicker the interface is, the easier it becomes to prepare a membrane of large transverse size.

Yang et al. [56] prepared GO in a solution with 2 mg/mL concentration. It was carried out through the evaporation method that removes the solvent, hence giving a surface holding characteristic to the self-assembled film of GO. It was observed that the thickness of GO can be controlled by controlling the time period and temperature of evaporation. GO with more carboxyl, hydroxyl, and epoxy clusters follow the layer-by-layer self-assembly route. In one case, the negative charge and carboxyl and the positive charge of the organic matter group was used to generate self-assembly. In another case, the reactivity of appropriate functional groups was employed to achieve self-assembly. For a carboxyl rich GO surface, the more probability there is of the creation of a negative charge for groups dispersed in water. Hence, the self-assembly becomes feasible by applying an electric field.

Researchers are currently focused on combining the properties of various nanomaterials to produce a single nanocomposite membrane with enhanced performance. Kou and Gao [57] successfully prepared a GO-SiO_2 nano-hybrid for employment in the applications of super hydrophilic coatings. Gao et al. [58] prepared a TiO_2 (P 25)–GO nanocomposite and found that the photocatalytic activity under the near violet-blue spectrum represents layer-by-layer self-assembly of GO on the top of TiO_2. The adsorption capacities of several other GO-based adsorbents can be further seen in Table S2 of supplementary file.

4. Metal and Metal Oxide Nanoparticles

Few nanoparticles of metals, such as silver (Ag), palladium (Pd), and gold (Au), have been intensively studied to be applied in wastewater treatment. Titanium decorated gold nanoparticles are effective in eliminating trichloroethane from groundwater. Tobiszewski et al. [59] showed that titanium nanoparticles catalysts show almost 2200 units better effectiveness than palladium alone. Nano silver in the form of colloidal and spun silver with 10–200 nm size exhibits high surface area and good antimicrobial properties. Due to this, silver nanoparticles are responsible for the removal of coli form microbes from wastewater [60].

TiO_2, Zinc Oxide (ZnO), and Cerium(IV) Oxide (i.e., CeO_2) metal oxide nanoparticles are employed for the degradation of various forms of organic pollutants that are usually present in the aqueous stream. Due to excellent surface area and photolytic properties, these metal oxide nanoparticles turn out to be a better option as photocatalysts for water and wastewater decontamination. Magnesium (Mg) and Magnesium Oxide (MgO) nanoparticles are helpful in the adsorption of biocides against Escherichia coli, Bacillus megaterium, and Bacillus subtillus (i.e., bacterial spores) [61]. Nano Copper(I) Oxide (i.e., Cu_2O) and TiO_2 electrodes exhibit coherent oxidation in electrocatalytic oxidation activity. These also show efficient COD removal rates [62]. Mei et al. [63] observed that upper layered crosslinked chitosan Ag–SiO_2 nanocomposites showed higher biocidal action for Escherichia coli and Staphylococcus. Ferrites with iron minerals, such as maghemite, goethite, akagneite, ferrihydrite, lepidocrocite, magnetite, and hematite, have been used for adsorption operations in wastewater treatment [64]. Oxides of iron (Fe) and titanium (Ti) acts as sorbents for the decontamination of wastewater from metal dopants. A Pd/Fe_3O_4 catalyst is used for dehalogenation in water and wastewater treatment [65].

4.1. Membranes Infused with Aluminium Nanoparticles

Aluminum based NPs can enhance the activity of membranes when fabricated with them. However, the addition of NPs has to be carried out very carefully as the excess of it can decline the adsorption capacity and membrane strength of the polymeric membranes. PVDF material forms asymmetric membranes of high permeability, good pore structures, and high porosity. It is also thermally stable and highly resistant to corrosion by various organic pollutants. PVDF membranes display good anti-oxidation properties; film-forming properties; and thermal, hydrolytic, and mechanical performance. These membranes have also been employed for ultrafiltration processes [66]. Besides all these benefits, PVDF membranes still require certain modifications. Various processes such as chemical grafting, surface modification, and physical blending can be used for modification purposes. Blending is relatively easier than other methods as it enables the inversion of phase easily. Further, when hydrophobic materials were added to dope solutions, the water permeability of the membrane increases with similar pore size and distribution. This is due to increasing pore density and hydrophilicity inside the pore surface of the membranes [67]. Ploymethyl methacrylate (PMMA) is another organic material that is used for blending with PVDF to enhance the pore side dispersion, structure, and penetration [68].

Inorganic fillers have shown potential properties to improve the effectiveness of PVDF membranes. Inorganic fillers result in the increase of membrane permeability and surface properties. A few of the inorganic fillers used so far includes silica, zirconium dioxide, and salts of lithium [7]. Yan et al. [69] demonstrated the modification of a PVDF membrane with inorganic nano-sized particles of aluminum oxide (Al_2O_3). The composite membrane was synthesized by the phase inversion method. The main aim of the study was to observe the effect of Al_2O_3 particle concentration on membrane morphology, hydrophilicity, mechanical performance, permeation flux, and anti-fouling properties. The following results were obtained from the experiment and characterizations:

- The permeate flux constantly increased with the addition of Al_2O_3 NPs; however, the trend reversed after the quantity of Al_2O_3 exceeded a certain limit. The trend of flux is represented in Figure 3.
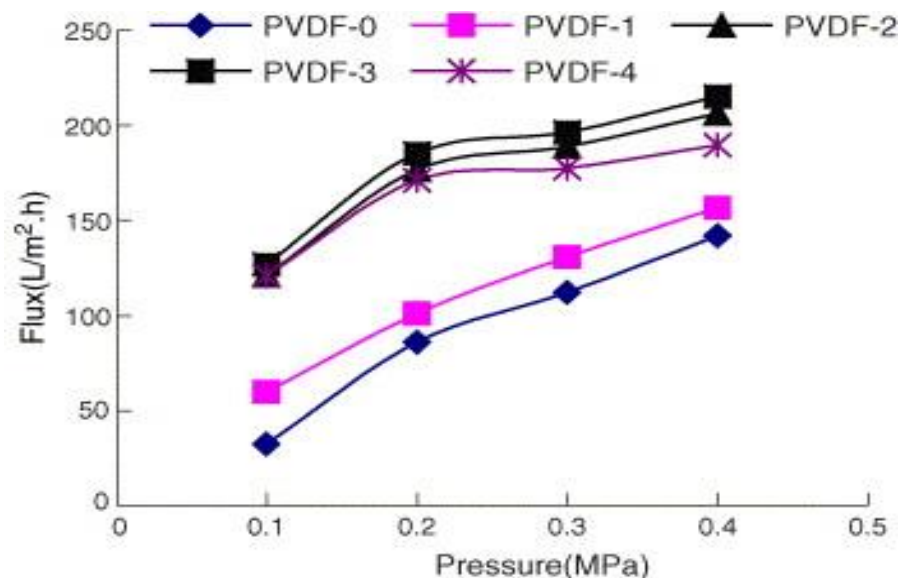

Figure 3. Distilled–H_2O fluxes of membranes having different compositions of nano-sized Al_2O_3 particles. Reprinted with permission from [69]. Copyright (2006) Elsevier B.V.

Thus, Al_2O_3 can highly influence the hydrophilicity of the PVDF membrane, hence increasing its surface area ratios. However, the flux cannot be improved after the Al_2O_3

concentration exceeds a fixed limit in casting drops. In reports, 2% by weight of nano Al_2O_3 particles were reported to be ideal.

- Further, the SEM micrographs of PVDF-0 and PVDF-2 membranes were studied. Micropores were found to be distributed on either side of the membrane without any difference among modified and unmodified membranes. Both membranes displayed finger-like pores along with sponge wall linkage. Thus it was concluded that Al_2O_3 NPs do not influence the surface structures, inner pores, and cross-section.
- It was also observed that, with an increase in Al_2O_3 particle concentration, the contact angle subsequently decreased. Other values such as porosity, rejection, and other cut-off value were not affected. This observation concludes that Al_2O_3 particles can improve the hydrophilicity of the PVDF membrane but have no influence on pore size and amount in the membrane.
- Figure 4 shows that Al_2O_3 NPs were mostly dispersed uniformly, with a few large bundles. These might be due to the overlapping or coalescing of particles in the membrane.
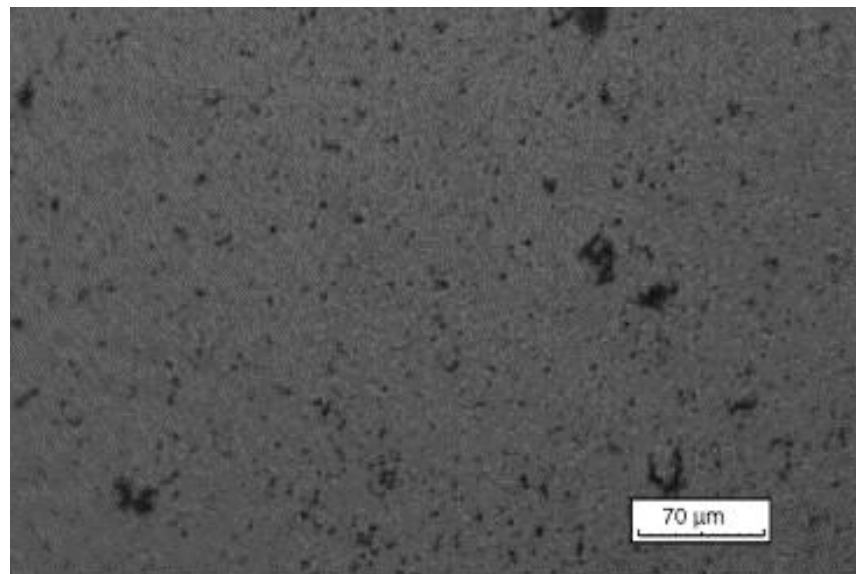

Figure 4. Differential coefficient interference pattern of Al_2O_3-particle distribution in the modified membrane. Reprinted with permission from [69]. Copyright (2006) Elsevier B.V.

Moreover, the mechanical properties of the membrane can also be enhanced with the appropriate addition of Al_2O_3 NPs. However, an excess concentration of NPs may also reduce the membrane elasticity, hence resulting in less elongation-at-break value.

4.2. Membranes Infused with Zirconium Nanoparticles

Zirconium dioxide is a potential compound for the synthesis of PVDF ultrafiltration membranes. The membrane properties can be effectively controlled by controlling the zirconium dioxide (ZrO_2) concentration or the PVDF solvent in ternary suspension. However, excessive ZrO_2 can also result in increased permeate flux [70]. When employed with sulfonated poly-ether-ketone, it reduces the permeability between water and methanol. This property makes ZrO_2 and poly-ether-ketone amalgamation a potential candidate to apply in the fuel cell. A fuel cell being an energy-efficient energy conversion device that utilizes polyelectrolyte membranes for mobile applications. However, storage is still an issue with fuel cell development. Alternatively, reforms can be used to produce hydrogen from methanol and gasoline. The reformer can then be extracted for gaining technical simplicity [71].

Nunes et al. [72] demonstrated the sulfonated poly-ether-ketone (SPEK) and sulfonated poly-ether-ether-ketone polymeric membranes. Inorganic branches were prepared

in a polymer-matrix through the hydrolysis of tetra-ethoxy silane (TEOS) and of 1-(3-triethoxysilyl propyl)-4,5-dihydroimidazole (I-silane). As shown in Figure 5, the modification by inorganic SiO_2 considerably reduced the permeability of the membrane.
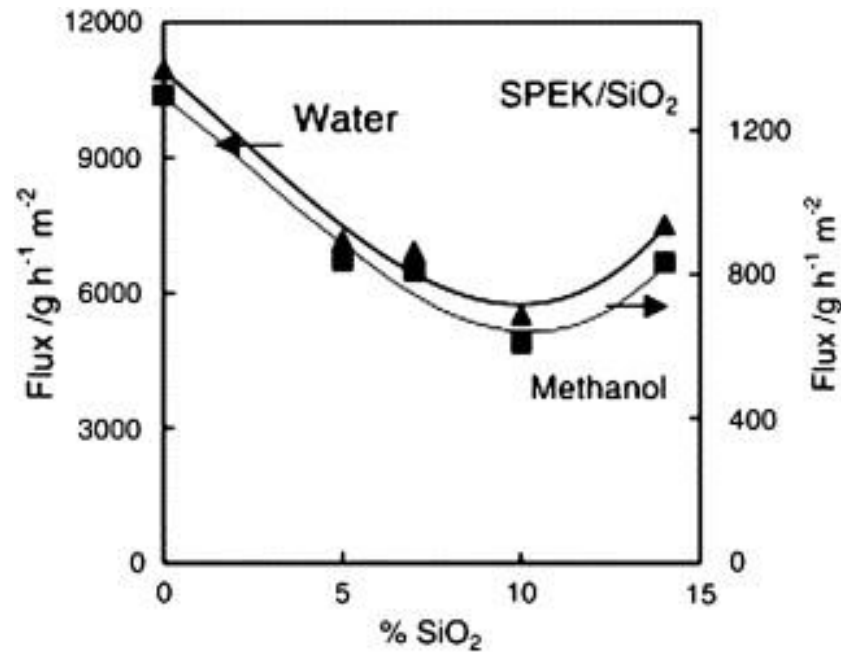

Figure 5. Methanol–H_2O flux in pervaporation experiments at 55 °C by modification of an SPEK membrane with hydrolyzed TEOS. Reprinted with permission from [72]. Copyright (2002) Elsevier Science B.V.

Further, it was observed that ZrO_2 and TiO_2 reduced the water-methanol permeability on its modification. Figure 6a demonstrates the water-methanol permeability reduction after they were modified with TiO_2, and only slight improvement was seen on pre-treating with 1,1′-carbonyl diimidazole (CDI), amino propylsilane (AS). Similarly, as shown in Figure 6b, distributing ZrO_2 particles in sulfonated poly-ether-ketone membranes highly reduced the methanol-water permeability. Furthermore, no additional enhancements were observed from pre-treatment with CDI and AS [72].
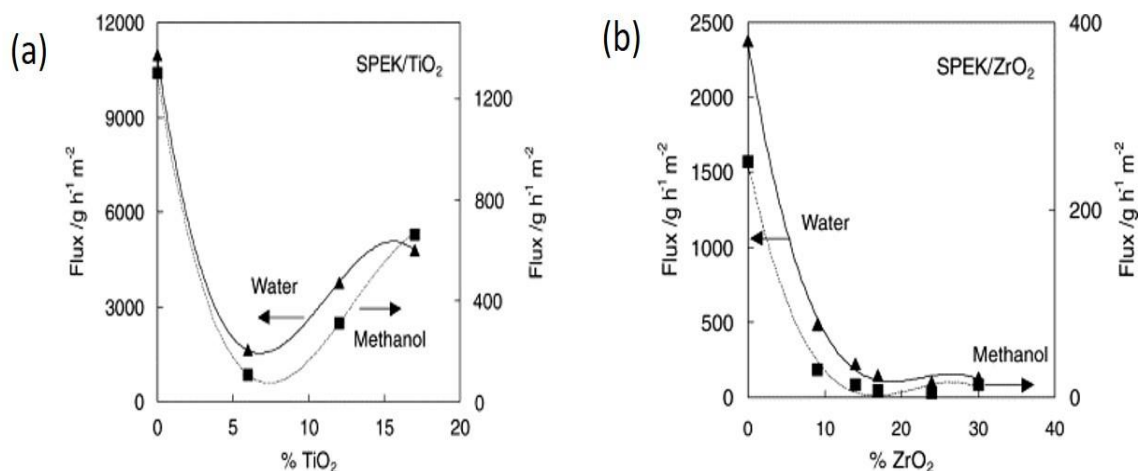

Figure 6. Methanol and water flux in pervaporation experiments at 55 °C post modification of a SPEK membrane with (**a**) TiO_2 and (**b**) ZrO_2. Reprinted with permission from [72]. Copyright (2002) Elsevier Science B.V.

Besides this, SEM (Figure 7) of the SPEK membrane enhanced with 22 wt.% TiO$_2$ displayed a good distribution of NPs, with inorganic networks been generated in the polymeric matrix through hydrolysis of TESO and I-silane.
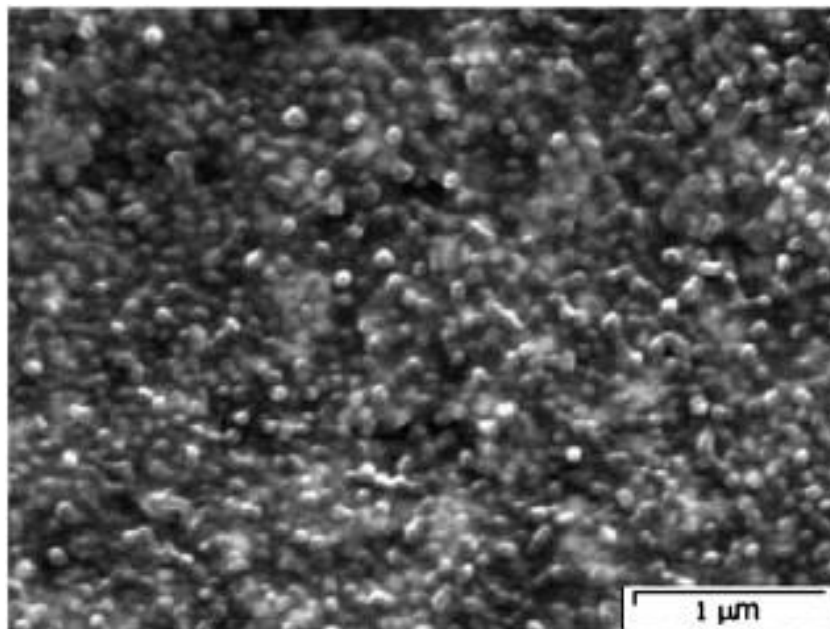

Figure 7. SEM of a SPEK membrane modified with 22 wt.% TiO$_2$. Reprinted with permission from [72]. Copyright (2002) Elsevier Science B.V.

It has also been reported that Nafion membranes doped with SiO$_2$ and ZrO$_2$ are capable of improving water retention and increase proton conductivity [73,74]. In another study by Pan et al. [75], synthesis of zirconia NPs of diameter 6.3 ± 0.5 nm is shown. NPs were prepared in situ in Nafion solution through hydrolysis and condensation of tetrabutylzirconate (TBZ). The result suggested that in situ zirconia NPs were homogeneously distributed in dispersion. Additionally, the suggested average diameter of NPs was nearly 6.3 ± 0.5. Further, all the adsorption peaks obtained through the FTIR spectrum of the hybrid membrane were without any shift of wave numbers. The zirconia addition does not disturb the crystallinity and structure of the molecules present in the membrane. Moreover, the Nafion molecules can also undergo self-assembly for the formation of zirconia particles by electrostatic interactions. The new Nafion-zirconia membrane showed improved water retention.

4.3. Membranes Infused with Silver Nanoparticles

Biofouling generally includes the microbial liberation of extracellular polymeric substances, which decreases the membrane flux and shortens the membrane life [76]. Fouling in the membrane is mostly controlled in pretreatment or chemical-based cleaning in backwashing. Introducing antimicrobial NPs in membranes can offer potential relief to biofouling. Silver NPs are considered amongst the best antibacterial materials that can be integrated within the polymer matrix of membranes [77]. Silver is also resistive towards corrosion and high toxicity. Moreover, silver NPs contribute well to water and wastewater purification applications. This is mainly because they successfully hamper waterborne microorganisms such as algae, fungi, and other microbes. Due to chemical and thermal stability, silver NPs and ions have been utilized in the fabrication of wastewater purification antibacterial membranes. Silver also combats a wide range of bacteria and has no adverse effect on humans [78,79]. In 1997, Davies et al. [80] reported that the antibacterial features of silver are due to its interactions with phosphorus and sulphur. When ionic silver and thiol groups interact to form S-Ag or disulphide bonds, the bacterial proteins and dimerize

DNA get damaged. It also interrupts the electron transport chain [81,82]. Furthermore, silver shows some antiviral characteristics to interact with the thiol group and DNA. Silver NPs also acts as a selective barrier to element transportation. These properties of silver enable its usage in various fields that includes the transportation of high-value products. Silver NPs and ions have been widely employed in water treatment applications, such as water purification membranes. Materials such as polyimide, polyamide, Poly(2-ethyl-2-oxazoline), and cellular acetate have all had silver NPs introduced into them to prepare efficient membranes.

Doping of silver-based materials into PMMA displays a sustainable membrane of higher selectivity. Besides this, silver-base materials have also been discussed in association with polymeric membranes such as polyamide membrane. Polyamide membrane is a popular material because of its high resistivity towards temperature and chemical compounds. Polyamides have bulky CF_3 groups that exhibit excellent film development and separation profiles [83]. To avoid the exhaustion of silver ions, a dry co-polyamide membrane was utilized with metal ions in the crown ether cavity. The examples are 4,4′-hexafluoro-isopropylidene diphthalic anhydride (6FDA) co-polyimides and 3,5-diamino benzoic acid (DABA). Further doping of silver ions in polymer materials considerably improves the selectivity, but with a reduction of permeability due to distortion of free volume. $AgBF_4$-infused membranes were found more selective than $AgNO_3$-infused membranes. However, the selectivity decreased with increasing feed pressure. in the long run, the reduction in separation factor was observed at constant feed pressure. In membranes without crown ethers, silver ions penetrate deeper into membrane structure due to there being more free volume available of the polymer. In such cases, membranes are comparatively stable. On the other hand, silver ions penetrate just up to the membrane layers in the presence of crown ether units [84].

Despite all these advantages of silver materials, researchers are still dubious about its commercial use. Increasing the use of silver NP systems may pose a health and environment risk of NPs. Silver infused polymeric materials used in the drinking water filtration process may lead to the leaching of silver NPs. This may be caused due to poor NP incorporation or physical damage to the membrane. Long-time exposure to silver may also lead to argyria, which results in blue-grey discoloration spots on the skin and other body organs. Besides this, in vitro examinations suggested that silver NPs cause damage to DNA structures and apoptosis in embryonic stem cells and fibroblasts of mouse [85].

4.4. Membranes Infused with Magnesium Nanoparticles

Membranes are continuously employed for gas separation applications in chemical and petrochemical industries. Separating hydrogen from hydrocarbons, removing carbon dioxide from natural gas, and nitrogen purification are some of the highly recognized industrial uses of membranes. However, polymeric membranes still suffer from selectivity issues, which restricts their future development [86]. Nanocomposite and facilitated transport membranes are two gas separation membrane generations that have the capability to be applied in purification and gas separation. The mechanism of interactions among magnesium oxide (MgO) and a few gas (e.g., CO_2) surfaces have motivated researchers to explore the capabilities of MgO infused membranes. Hosseini et al. [87] fabricated a flat nanocomposite membrane by infusing MgO NPs into a Matrimid polymer matrix. MgO NPs enhanced the permeability and effected the selectivity of the membrane. As shown in Figure 8, it is observed that the permeability of the modified membrane is relatively higher than the pristine Matrimid membrane. Additionally, there is a regular rise in permeability with increasing MgO concentration.
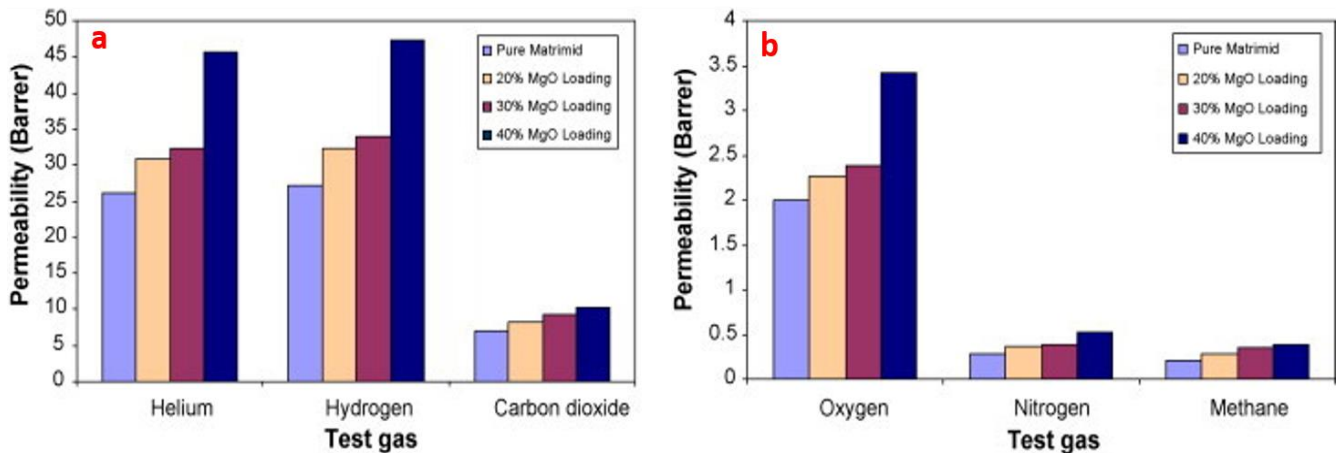
Figure 8. Comparison between gas permeability of pure Matrimid and its nanocomposite membranes having different concentrations of MgO NPs; (**a**) shows the comparison of helium, hydrogen, and carbon dioxide; (**b**) shows the comparison of oxygen, nitrogen, and methane. Reprinted with permission from [87]. Copyright (2007) Elsevier B.V.

The average increase in gas permeability is nearly 70% from using 40 wt.% MgO particles. Clearly, the highly porous magnesium oxide NPs occupy the space in the dense structure of polymeric chains and hence increases the gas permeability.

4.5. Membranes Infused with Copper Nanoparticles

Copper was initially used in the sterilization of injuries and water back in 2000 BCE in ancient Egypt. Romanians also utilized it to manufacture hygienic utensils. Phoenician ship manufacturers installed copper strips to the hulls of a ship to prevent fouling and enhance the maneuverability of the ship. In WW II, Japanese people added copper to canteens to battle dysentery [88]. Copper was also utilized as a fungicide in the late 19th century [89]. Copper NPs can easily be oxidized into copper oxides. To prevent oxidation, argon and nitrogen inert atmospheres can be employed with other organic coatings [90]. The dependence of the mechanical and physical characteristics of PVDF-Cu composite on copper concentration was studied by utilizing the Cambridge Engineering Selector (CES) software. Bassyouni et al. [91] listed the various findings of CSE in a tabular form. The various methods that are currently employed for copper NPs synthesis include chemical, biological, and physical.

The biological technique is very much similar to the chemical technique; the only difference is that it utilizes biomolecules for synthesizing NPs through the reduction of metallic ions. Another method of copper NPs synthesis, i.e., physical process, enables the synthesis of copper NPs of different sizes and structures. However, the process utilizes expensive machinery and also produces low-quality particles compared to chemical processes.

Palza et al. [92] showed the direct relation of NP's antibacterial properties of Cu^{2+} with the particle size. When NPs of diameter 10 nm are introduced into polypropylene matrix, the ion release rapidly increases. However, for particles with a diameter of 45 μm, the ion release increases slowly. Nanocomposites with 5 v/v% copper happen to remove 99.8% Staphylococcus aureus after 1 h. Copper NPs, copper oxide NPs, and copper ions attack different species of bacteria to act as an antimicrobial material. These are also relatively much more affordable than silver.

Ben-Sasson et al. [93] used electrostatic interactions to physically embed positive poluethylenimine-modified copper NPs onto a negative thin film composite. Because PEI is a good capping reagent to monitor copper NP size, it provides a stable and uniform film and lowers the bacterial concentration up to 80–95%. Further, in order to modify the surface, Ma et al. [94] prepared a technique known as the spray/spin assisted layer-by-layer (SSLbL) technique. In order to control biofouling, the SSLbL method was employed to modify the thin film composite membrane surface with the help of copper NPs. Another

strategy, called the swift strategy, uses reduced graphene oxide-copper (rGOC) nanocomposite to co-deposit it along polydopamine (PDA) on a hydrolyzed PAN UF membrane [95]. The characterization demonstrated that copper NPs are uniformly dispersed around the rGO surface. Further, the bridging across the voids of the UF membrane improves the water permeability and dye removal capacity. Almost 97.9% Escherichia coli was observed to become inactive by using multi-functional PDA-rGOC later for bridging. Hence, swift and co-deposition methods emerged as a possible solution for loading antibacterial nanomaterials onto membrane surfaces.

4.6. Outlook

As discussed in the above sections, PVDF is the most favorable material to fabricate membranes. However, it is immediately contaminated with proteins and other wastewater contaminants during water treatment, hence resulting in a sharp decrease in membrane flux. Therefore, infusing membranes with metal and metal oxide NPs improves their chemical and physical properties. Silver represents an ideal candidate to reduce membrane biofouling. However, incorporation of silver NPs may also lead to the reduction of void volume and the permeability of the membranes.

In drinkable water purposes, nanoparticles should be controlled carefully due to their toxic properties. Moreover, the amount of NPs and polymeric materials must be optimized to manufacture economical and high performance membranes in the future. Further merits and demerits of different metal/metal oxide polymeric membranes can be seen fin Table S3, provided in the supplementary material.

5. Zwitter-Ion Based Polymeric Membranes

Antifouling properties of zwitter-ionic materials follows two main paths when the surface is below water. The first one includes hydration shell formation through electrostatic interactions. This acts as an effective barrier for foulants and blocks them from making direct contact with the surface [96]. According to thermodynamics, foulants require high energy to break the hydration shell. Therefore, the maximum Gibbs free energy present on the hydrophilic surface is higher than unmodified surfaces. This significantly decreases the possibility of adsorption taking place. As compared to polyethylene glycol (PEG) and derivatives, zwitter-ionic materials configure a thick and denser hydration shell. This is mainly because the PEG molecular chain contains a repeated $-CH_2CH_2O-$ units and also every unit contains an oxygen atom joined with a water molecule through hydrogen bonding. Zwitter-ionic chains have both positive as well as negatively charged groups, which are bonded to a maximum of eight water molecules with the help of the electrostatic force of interactions [97]. In the case of macromolecular biological foulants, the hydrophilic materials shell creates a small water atmosphere and liberates water to maintain the conformation, hence giving materials the lesser adsorption tendencies and high biocompatibility [98].

The second way in which zwitter-ionic materials show antifouling actions includes the effect of steric hindrance. In zwitter-ionic polymers, the steric effect works quite similarly to hydrophilic polymer chains, having higher embargo volume by virtue of motility and hydrophobicity. Chang et al. [99] postulated that the minimized dipole of zwitter-ions and the balanced charge are two important factors for antifouling. Zwitter-ionic materials having both the conditions to repulse charge proteins by electrostatic repulsions. He also stated that zwitter-ionic heads with an anti-parallel orientation work to minimize the dipole. Furthermore, the theory was proved correct through various molecular simulation calculations. Subsequent experiments were performed for protein absorption using zwitter-ionic polymers with an unequal charge. The outcome showed that zwitter-ionic polymers with unequal charges show reduced antifouling properties. The practical application of this is having control upon the charge distribution when zwitter-ionic materials are employed as antifouling compounds. Another implication is that membrane may also be of lower surface packing, hence lowering the total number of water molecules of the polymeric

chain. Chang et al. [99] got the model to work on interface surfaces. However, the same was also seen to be applied in the case of rough and porous membrane surfaces. Further, a multilayered zwitter-ionic polymer was developed. The initial layer had the lowest foiling, then the higher loading in the second layer. The whole arrangement shows higher anti-fouling properties than single-layer arrangements [100]. Chang et al. [99] then showed that an increase in density and zwitter-ionic material length would enhance the protein resistance. In 2015, the same group of researchers used molecular modelling and simulations to study the structural properties and their relationships with zwitter-ionic materials on a molecular level. Finally, they proposed that good anti-fouling characteristics are assisted by strong hydration, moderate self-associations, and lower protein interactions [101].

The surrounding environment conditions in which zwitter-ionic materials operate also play a major role in its anti-fouling activity. In conditions where positive and negative charges have strong interactivity, the zwitter-ionic polymers tend to aggregate and hence give more surface to external hydrophobic and hydrocarbon groups. This eliminated the steric hindrance and hydration shell. Conversely, on adding a small amount of salt, the screening process protects the positive and negative charge interactions. This expands the polymer chain and creates a strong steric hindrance with dense hydration shell [101].

A new technique is proposed for preparing high permissive polyamide thin-film nanocomposite membranes (TFNMs) by embedding soft zwitter-ionic co-polymers onto sodium carboxy-methyl cellulose. This technique shows improved water permeability and fouling resistance. The synthesized zwitter-ionic nano-gel (ZNG) shows good interactions with organic particles and polymer grids. Organic materials (i.e., antibiotics) and salts (i.e., NaCl, MgCl, Na_2SO_4, etc.) can be ideally separated with high water permeation, meaning that ZNG thin-film nanocomposite membranes have the potential of separating organic pollutants and salts. This examination provides a comprehensive approach to the structure and separation efficiency of the membrane, allowing us to further explore different ways to improve TFN nano-filtration membranes [102].

6. Zeolite-Based Polymeric Membranes

Various studies have shown zeolites as a potential material for permeability and selectivity applications. Liu et al. [103] experimented with the performance of PSf membrane by incorporating zeolite 4A. This experiment studied the influence of zeta potential and its content and the micro-channel dimensions and particle size of UF membranes. Zeolite 4A offers a rough surface and hence enhances the hydrophobicity. Introducing Zeolite 4A accurately into a PSf membrane creates swift nanoscale water routed for its flow. This also creates a negatively charged surface, with higher density and roughness. These membranes displayed good mechanical and thermal stability and improved fouling resistance.

Han et al. [104] experimented with the effect of NaA-zeolite particles in UF membrane composite with poly-(phthalazinone ether sulfone ketone) (PPESK). PPESK is a chemically and thermally stable compound with the good, mechanical strength required to prepare an efficient UF membrane. Because PPESK is hydrophobic, it has certain limitations in the aqueous phase. On the contrary, NaA-zeolite is a hydrophilic material used to improve the virtues of PPESK. On examination, membranes displayed high hydrophobicity, water permeability, and antifouling capacity with 3 wt.% NaA. Additionally, the PEG 6000 rejection was 77.9% and 96.8% in the absence and presence of NaA-zeolite particles, respectively. However, the flux decreased from 340 to 246 l/m^{2}h. It was further concluded that NaA/PPESK UF-membranes have better performance than commercially prepared UF membranes.

He et al. [105] further experimented with UF-PVDF membranes by adding an MCM-41 zeolite particles into it. These membranes have high permeability and mechanical strength. The highest mechanical strength of the composite reaches 3 wt.% zeolite NPs, with 71.75 MPa tensile strength. In comparison to this, pristine UF-PVDF membranes show only 22.5 MPa tensile strength. Additionally, the permeability of zeolite NPs enhanced UF membranes increased from 91,200 M/m^{2}h bar to 118,900 L/m^{2}h bar.

Leo et al. [106] used SAPO-44 as a filler against the fouling generated from the humid acid and organic matter present in PSf-UF membranes. Different samples of (Sf/PVA/SAPO-44)-UF membrane were prepared for the examinations. The results demonstrated that a membrane containing 15 wt.% SAPO-44 zeolite shows the highest water flux, with a 164% increase as compared to pure membrane. At 15 wt.% SAPO-44, 80% permeate flux was able to be maintained throughout the operation. On the other hand, there was a slight drop in permeability and water flux with 20 wt.% SAPO-44.

Zeolite membranes have also been widely employed in applications such as acid separation, alcohol dehydration, and organic/inorganic separations [107]. A pervaporation process is employed for separation purposes. It is used where separations are comparatively difficult with conventional techniques. Kunnakorn et al. [108] identified different ways of improving the performance of NaA-zeolite membranes under pervaporation with a water-ethanol mixture. Alumina was used as a support to modify the zeolite membrane. The experiment produced a stable membrane with high separation efficiency. The membrane showed filtration for 130 h with water flux ranging between 0.4–1.0 kg/m^{2}h.

7. Conclusions

Finally, the activity of adsorption of dendrimers relies over the nature and physicochemical characteristics of adsorbents. Surface and functionalization are two critical parameters in determining the operational efficiency of new adsorbents. Both specific surface area and intrinsic cavities can bond with pollutants through different interactions. Dendrimers can also be modified as per the requirement of targeted pollutants. They are less toxic, biocompatible, and are potential materials for water purification. Carbon-based nanomaterials are presently dominating as adsorbents for water treatment. Graphene provides the potential for preparing size-selective membrane due to its excellent mechanical properties and atomic thickness. In CNT and graphene-based membranes, a relatively lower number of components are needed for its operation. In upcoming research, combing these carbon-based nanomaterials with other compounds is highly preferred to develop a next-generation water treatment system. Metal and metal oxide NPs are superior because they already have well-developed synthesis paths. They enhance membrane hydrophilicity and are economical to use. Copper NPs can deactivate almost 90% of live bacteria from untreated water. Silica NPs/PSf membranes can handle a good amount of tensile force along with its activity as an antifouling membrane. Zwitter-ionic materials have shown potential applications in antifouling membranes through steric hindrance effects.

Moreover, the impacts and implications of environmental nanomaterials must be focused on; their preparation through green chemistry needs to be studied to eliminate their adverse environmental effects. Guidelines should be strictly followed about the harmful effects of nanomaterials on human and aquatic habitats.

Conflicts of Interest: The authors declare no conflict of interest.

References

1. Shannon, M.A.; Bohn, P.W.; Elimelech, M.; Georgiadis, J.G.; Mariñas, B.J.; Mayes, A.M. Science and technology for water purification in the coming decades. *Nanosci. Technol.* **2009**, *452*, 337–346. [CrossRef]
2. Babbar, R.; Arya, D.; Joshi, H. A Proposed Decision Support System for River Water Quality Management in India. *J. Decis. Syst.* **2009**, *18*, 411–427. [CrossRef]
3. Zhang, J.; Chen, G.; Ma, Y.; Xu, M.; Qin, S.; Liu, X.; Feng, H.; Hou, L. Purification of pickling wastewater from the steel industry using membrane filters: Performance and membrane fouling. *Environ. Eng. Res.* **2020**, *27*, 106–115. [CrossRef]
4. Ahmad, N.A.; Goh, P.S.; Wong, K.C.; Zulhairun, A.K.; Ismail, A.F. Enhancing desalination performance of thin film composite membrane through layer by layer assembly of oppositely charged titania nanosheet. *Desalination* **2020**, *476*, 114167. [CrossRef]
5. Han, K.N.; Yu, B.Y.; Kwak, S.-Y. Hyperbranched poly(amidoamine)/polysulfone composite membranes for Cd(II) removal from water. *J. Membr. Sci.* **2012**, *396*, 83–91. [CrossRef]
6. Park, S.; Yang, E.; Park, H.; Choi, H. Fabrication of functionalized halloysite nanotube blended ultrafiltration membranes for high flux and fouling resistance. *Environ. Eng. Res.* **2019**, *25*, 771–778. [CrossRef]
7. Ng, L.Y.; Mohammad, A.W.; Leo, C.P.; Hilal, N. Polymeric membranes incorporated with metal/metal oxide nanoparticles: A comprehensive review. *Desalination* **2013**, *308*, 15–33. [CrossRef]
8. Misdan, N.; Ismail, A.F.; Hilal, N. Recent advances in the development of (bio)fouling resistant thin film composite membranes for desalination. *Desalination* **2016**, *380*, 105–111. [CrossRef]
9. Ren, Y.; Zhu, J.; Cong, S.; Wang, J.; Van der Bruggen, B.; Liu, J.; Zhang, Y. High flux thin film nanocomposite membranes based on porous organic polymers for nanofiltration. *J. Membr. Sci.* **2019**, *585*, 19–28. [CrossRef]
10. Ortega, M.; Merino, A.G.; Fraile-Martínez, O.; Recio-Ruiz, J.; Pekarek, L.; Guijarro, L.G.; García-Honduvilla, N.; Álvarez-Mon, M.; Buján, J.; García-Gallego, S. Dendrimers and Dendritic Materials: From Laboratory to Medical Practice in Infectious Diseases. *Pharmaceutics* **2020**, *12*, 874. [CrossRef]
11. Bethi, B.; Sonawane, S.H.; Bhanvase, B.A.; Gumfekar, S.P. Nanomaterials-based advanced oxidation processes for wastewater treatment: A review. *Chem. Eng. Process. Process. Intensif.* **2016**, *109*, 178–189. [CrossRef]
12. Barakat, M.A.; Ramadan, M.H.; Alghamdi, M.A.; Algarny, S.S.; Woodcock, H.L.; Kuhn, J.N. Remediation of Cu (II), Ni (II), and Cr (III) ions from simulated wastewater by dendrimer/titania composites. *J. Environ. Manag.* **2013**, *117*, 50–57. [CrossRef]
13. Barakat, M.; Ramadan, M.; Kuhn, J.; Woodcock, H. Equilibrium and kinetics of Pb2+adsorption from aqueous solution by dendrimer/titania composites. *Desalination Water Treat.* **2014**, *52*, 5869–5875. [CrossRef]
14. Castillo, V.A.; Barakat, M.A.; Ramadan, M.H.; Woodcock, H.L.; Kuhn, J.N. Metal ion remediation by polyamidoamine dendrimers: A comparison of metal ion, oxidation state, and titania immobilization. *Int. J. Environ. Sci. Technol.* **2014**, *11*, 1497–1502. [CrossRef]
15. Chou, C.-M.; Lien, H.-L. Dendrimer-conjugated magnetic nanoparticles for removal of zinc (II) from aqueous solutions. *J. Nanoparticle Res.* **2011**, *13*, 2099–2107. [CrossRef]
16. Yen, C.-H.; Lien, H.-L.; Chung, J.-S.; Yeh, H.-D. Adsorption of precious metals in water by dendrimer modified magnetic nanoparticles. *J. Hazard. Mater.* **2017**, *322*, 215–222. [CrossRef] [PubMed]
17. Liang, X.; Ge, Y.; Wu, Z.; Qin, W. DNA fragments assembled on polyamidoamine-grafted core-shell magnetic silica nanoparticles for removal of mercury(II) and methylmercury(I). *J. Chem. Technol. Biotechnol.* **2017**, *92*, 819–826. [CrossRef]
18. Kim, K.-J.; Park, J.-W. Stability and reusability of amine-functionalized magnetic-cored dendrimer for heavy metal adsorption. *J. Mater. Sci.* **2017**, *52*, 843–857. [CrossRef]
19. Pourjavadi, A.; Abedin-Moghanaki, A.; Hosseini, S.H. Synthesis of poly(amidoamine)-graft-poly(methyl acrylate) magnetic nanocomposite for removal of lead contaminant from aqueous media. *Int. J. Environ. Sci. Technol.* **2016**, *13*, 2437–2448. [CrossRef]
20. Zhou, S.L.; Li, J.; Hong, G.-B.; Chang, C.-T. Dendrimer Modified Magnetic Nanoparticles as Adsorbents for Removal of Dyes. *J. Nanosci. Nanotechnol.* **2013**, *13*, 6814–6819. [CrossRef]
21. Zarghami, Z.; Akbari, A.; Latifi, A.M.; Amani, M.A. Design of a new integrated chitosan-PAMAM dendrimer biosorbent for heavy metals removing and study of its adsorption kinetics and thermodynamics. *Bioresour. Technol.* **2016**, *205*, 230–238. [CrossRef]
22. Zhao, J.; Zhang, X.; He, X.; Xiao, M.; Zhang, W.; Lu, C. A super biosorbent from dendrimer poly(amidoamine)-grafted cellulose nanofibril aerogels for effective removal of Cr(vi). *J. Mater. Chem. A* **2015**, *3*, 14703–14711. [CrossRef]
23. Wang, P.; Ma, Q.; Hu, D.; Wang, L. Removal of Reactive Blue 21 onto magnetic chitosan microparticles functionalized with polyamidoamine dendrimers. *React. Funct. Polym.* **2015**, *91*, 43–50. [CrossRef]
24. Algarra, M.; Vázquez, M.I.; Alonso, B.; Casado, C.M.; Casado, J.; Benavente, J. Characterization of an engineered cellulose based membrane by thiol dendrimer for heavy metals removal. *Chem. Eng. J.* **2014**, *253*, 472–477. [CrossRef]
25. Yuan, Y.; Zhang, G.; Li, Y.; Zhang, G.; Zhang, F.; Fan, X. Poly(amidoamine) modified graphene oxide as an efficient adsorbent for heavy metal ions. *Polym. Chem.* **2013**, *4*, 2164–2167. [CrossRef]
26. Zhang, F.; Wang, B.; He, S.; Man, R. Preparation of Graphene-Oxide/Polyamidoamine Dendrimers and Their Adsorption Properties toward Some Heavy Metal Ions. *J. Chem. Eng. Data* **2014**, *59*, 1719–1726. [CrossRef]
27. Xiao, W.; Yan, B.; Zeng, H.; Liu, Q. Dendrimer functionalized graphene oxide for selenium removal. *Carbon* **2016**, *105*, 655–664. [CrossRef]

28. Iannazzo, D.; Pistone, A.; Ziccarelli, I.; Espro, C.; Galvagno, S.; Giofrè, S.; Romeo, R.; Cicero, N.; Bua, G.D.; Lanza, G.; et al. Removal of heavy metal ions from wastewaters using dendrimer-functionalized multi-walled carbon nanotubes. *Environ. Sci. Pollut. Res.* **2017**, *24*, 14735–14747. [CrossRef]

29. Hayati, B.; Maleki, A.; Najafi, F.; Daraei, H.; Gharibi, F.; McKay, G. Super high removal capacities of heavy metals (Pb 2+ and Cu 2+) using CNT dendrimer. *J. Hazard. Mater.* **2017**, *336*, 146–157. [CrossRef]

30. Xu, Y.; Zhao, D. Removal of Copper from Contaminated Soil by Use of Poly(amidoamine) Dendrimers. *Environ. Sci. Technol.* **2005**, *39*, 2369–2375. [CrossRef] [PubMed]

31. Gajjar, D.; Patel, R.; Patel, H.; Patel, P.M. Designing of Triazine Based Dendrimer and its Application in Removal of Heavy Metal Ions from Water. *Chem. Sci. Trans.* **2014**, *3*, 897–908. [CrossRef]

32. Xu, Y.; Zhao, D. Removal of Lead from Contaminated Soils Using Poly(amidoamine) Dendrimers. *Ind. Eng. Chem. Res.* **2006**, *45*, 1758–1765. [CrossRef]

33. Taleb, M.A.; Elsigeny, S.M.; Ibrahim, M.M. Radiation synthesis and characterization of polyamidoamine dendrimer macro-molecules with different loads of nickel salt for adsorption of some metal ion. *Radiat. Phys. Chem.* **2007**, *76*, 1612–1618. [CrossRef]

34. Beraa, A.; Hajjaji, M.; Laurent, R.; Delavaux-Nicot, B.; Caminade, A.-M. Removal of chromate from aqueous solutions by dendrimers-clay nanocomposites. *Desalination Water Treat.* **2016**, *57*, 14290–14303. [CrossRef]

35. Rao, N.; Singh, R.; Bashambu, L. Carbon-based nanomaterials: Synthesis and prospective applications. *Mater. Today Proc.* **2021**, *44*, 608–614. [CrossRef]

36. Geng, B.; Jin, Z.; Li, T.; Qi, X. Kinetics of hexavalent chromium removal from water by chitosan-Fe0 nanoparticles. *Chemosphere* **2009**, *75*, 825–830. [CrossRef]

37. Cheung, W.; Szeto, Y.; McKay, G. Enhancing the adsorption capacities of acid dyes by chitosan nano particles. *Bioresour. Technol.* **2009**, *100*, 1143–1148. [CrossRef]

38. Hinds, B.J.; Chopra, N.; Rantell, T.; Andrews, R.; Gavalas, V.; Bachas, L. Aligned Multiwalled Carbon Nanotube Membranes. *Science* **2004**, *303*, 62–65. [CrossRef]

39. Hummer, G.; Rasaiah, J.C.; Noworyta, J.P. Water conduction through the hydrophobic channel of a carbon nanotube. *Nature* **2001**, *414*, 188–190. [CrossRef]

40. Thomas, J.A.; McGaughey, A.J.H. Water Flow in Carbon Nanotubes: Transition to Subcontinuum Transport. *Phys. Rev. Lett.* **2009**, *102*, 184502. [CrossRef] [PubMed]

41. Chen, K.; Li, J.; Zhang, L.; Xing, R.; Jiao, T.; Gao, F.-M.; Peng, Q. Facile synthesis of self-assembled carbon nanotubes/dye composite films for sensitive electrochemical determination of Cd(II) ions. *Nanotechnology* **2018**, *29*, 445603. [CrossRef] [PubMed]

42. Chan, Y.; Hill, J.M. Modeling on ion rejection using membranes comprising ultra-small radii carbon nanotubes. *Eur. Phys. J. B* **2012**, *85*, 1–7. [CrossRef]

43. Farid, M.U.; Khanzada, N.K.; An, A.K. Understanding fouling dynamics on functionalized CNT-based membranes: Mechanisms and reversibility. *Desalination* **2019**, *456*, 74–84. [CrossRef]

44. Wang, H.; Zhang, D.; Yan, T.; Wen, X.; Shi, L.; Zhang, J. Graphene prepared via a novel pyridine–thermal strategy for capacitive deionization. *J. Mater. Chem.* **2012**, *22*, 23745–23748. [CrossRef]

45. Stankovich, S.; Dikin, D.A.; Compton, O.C.; Dommett, G.H.B.; Ruoff, R.S.; Nguyen, S.T. Systematic Post-assembly Modification of Graphene Oxide Paper with Primary Alkylamines. *Chem. Mater.* **2010**, *22*, 4153–4157. [CrossRef]

46. Li, D.; Müller, M.B.; Gilje, S.; Kaner, R.B.; Wallace, G.G. Processable aqueous dispersions of graphene nanosheets. *Nat. Nanotechnol.* **2008**, *3*, 101–105. [CrossRef] [PubMed]

47. Huang, H.; Ying, Y.; Peng, X. Graphene oxide nanosheet: An emerging star material for novel separation membranes. *J. Mater. Chem. A* **2014**, *2*, 13772–13782. [CrossRef]

48. Lu, J.; Yang, J.-X.; Wang, J.; Lim, A.; Wang, S.; Loh, K.P. One-Pot Synthesis of Fluorescent Carbon Nanoribbons, Nanoparticles, and Graphene by the Exfoliation of Graphite in Ionic Liquids. *ACS Nano* **2009**, *3*, 2367–2375. [CrossRef]

49. Peng, L.; Xu, Z.; Liu, Z.; Wei, Y.; Sun, H.; Zhao, X.; Gao, C. An iron-based green approach to 1-h production of single-layer graphene oxide. *Nat. Commun.* **2015**, *6*, 1–9. [CrossRef]

50. Bao, C.; Song, L.; Xing, W.; Yuan, B.; Wilkie, C.A.; Huang, J.; Guo, Y.; Hu, Y. Preparation of graphene by pressurized oxidation and multiplex reduction and its polymer nanocomposites by masterbatch-based melt blending. *J. Mater. Chem.* **2012**, *22*, 6088–6096. [CrossRef]

51. Wang, X.; Xiong, Z.; Liu, Z.; Zhang, T. Exfoliation at the Liquid/Air Interface to Assemble Reduced Graphene Oxide Ultrathin Films for a Flexible Noncontact Sensing Device. *Adv. Mater.* **2015**, *27*, 1370–1375. [CrossRef]

52. Chen, X.; Liu, G.; Zhang, H.; Fan, Y. Fabrication of graphene oxide composite membranes and their application for pervaporation dehydration of butanol. *Chin. J. Chem. Eng.* **2015**, *23*, 1102–1109. [CrossRef]

53. Tsou, C.-H.; An, Q.-F.; Lo, S.-C.; De Guzman, M.; Hung, W.-S.; Hu, C.-C.; Lee, K.-R.; Lai, J.-Y. Effect of microstructure of graphene oxide fabricated through different self-assembly techniques on 1-butanol dehydration. *J. Membr. Sci.* **2015**, *477*, 93–100. [CrossRef]

54. Han, Y.; Jiang, Y.; Gao, C. High-Flux Graphene Oxide Nanofiltration Membrane Intercalated by Carbon Nanotubes. *ACS Appl. Mater. Interfaces* **2015**, *7*, 8147–8155. [CrossRef] [PubMed]

55. Sun, H.; Chen, G.; Huang, R.; Gao, C. A novel composite nanofiltration (NF) membrane prepared from glycolchitin/poly (acrylonitrile) (PAN) by epichlorohydrin cross-linking. *J. Membr. Sci.* **2007**, *297*, 51–58. [CrossRef]

56. Yang, L.; Tang, B.; Wu, P. UF membrane with highly improved flux by hydrophilic network between graphene oxide and brominated poly(2,6-dimethyl-1,4-phenylene oxide). *J. Mater. Chem. A* **2014**, *2*, 18562–18573. [CrossRef]
57. Kou, L.; Gao, C. Making silicananoparticle-covered graphene oxide nanohybrids as general building blocks for large-area superhydrophilic coatings. *Nanoscale* **2011**, *3*, 519–528. [CrossRef] [PubMed]
58. Gao, Y.; Hu, M.; Mi, B. Membrane surface modification with TiO2–graphene oxide for enhanced photocatalytic performance. *J. Membr. Sci.* **2014**, *455*, 349–356. [CrossRef]
59. Tobiszewski, M.; Namiesnik, J. Abiotic degradation of chlorinated ethanes and ethenes in water. *Environ. Sci. Pollut. Res.* **2012**, *19*, 1994–2006. [CrossRef]
60. Jain, P.; Pradeep, T. Potential of silver nanoparticle-coated polyurethane foam as an antibacterial water filter. *Biotechnol. Bioeng.* **2005**, *90*, 59–63. [CrossRef]
61. Bashambu, L.; Singh, R.; Verma, J. Metal/metal oxide nanocomposite membranes for water purification. *Mater. Today Proc.* **2021**, *44*, 538–545. [CrossRef]
62. Chang, J.-H.; Yang, T.-J.; Tung, C.-H. Performance of nano- and nonnano-catalytic electrodes for decontaminating municipal wastewater. *J. Hazard. Mater.* **2009**, *163*, 152–157. [CrossRef]
63. Mei, N.; Xuguang, L.; Jinming, D.; Husheng, J.; Liqiao, W.; Bingshe, X. Antibacterial activity of chitosan coated Ag-loaded nano-SiO2 composites. *Carbohydr. Polym.* **2009**, *78*, 54–59. [CrossRef]
64. Babu, A.T.; Antony, R. Green synthesis of silver doped nano metal oxides of zinc & copper for antibacterial properties, adsorption, catalytic hydrogenation & photodegradation of aromatics. *J. Environ. Chem. Eng.* **2019**, *7*, 102840. [CrossRef]
65. Hildebrand, H.; Mackenzie, K.; Kopinke, F.-D. Pd/Fe3O4 nano-catalysts for selective dehalogenation in wastewater treatment processes—Influence of water constituents. *Appl. Catal. B Environ.* **2009**, *91*, 389–396. [CrossRef]
66. Malekizadeh, A.; Schenk, P.M. High flux water purification using aluminium hydroxide hydrate gels. *Sci. Rep.* **2017**, *7*, 1–13. [CrossRef]
67. Jung, B. Preparation of hydrophilic polyacrylonitrile blend membranes for ultrafiltration. *J. Membr. Sci.* **2004**, *229*, 129–136. [CrossRef]
68. Nunes, S.P.; Peinemann, K.V. Ultrafiltration membranes from PVDF/PMMA blends. *J. Membr. Sci.* **1992**, *73*, 25–35. [CrossRef]
69. Yan, L.; Li, Y.S.; Xiang, C.B.; Xianda, S. Effect of nano-sized Al2O3-particle addition on PVDF ultrafiltration membrane performance. *J. Membr. Sci.* **2006**, *276*, 162–167. [CrossRef]
70. Xu, Z.-K.; Xiao, L.; Wang, J.-L.; Springer, J. Gas separation properties of PMDA/ODA polyimide membranes filling with polymeric nanoparticles. *J. Membr. Sci.* **2002**, *202*, 27–34. [CrossRef]
71. Singh, R.; Singh, M.; Gautam, S. Hydrogen economy, energy, and liquid organic carriers for its mobility. *Mater. Today Proc.* **2020**. [CrossRef]
72. Nunes, S. Inorganic modification of proton conductive polymer membranes for direct methanol fuel cells. *J. Membr. Sci.* **2002**, *203*, 215–225. [CrossRef]
73. Vallejo, E.; Pourcelly, G.; Gavach, C.; Mercier, R.; Pineri, M. Sulfonated polyimides as proton conductor exchange membranes. Physicochemical properties and separation H+/Mz+ by electrodialysis comparison with a perfluorosulfonic membrane. *J. Membr. Sci.* **1999**, *160*, 127–137. [CrossRef]
74. Jalani, N.H.; Dunn, K.; Datta, R. Synthesis and characterization of Nafion®-MO2 (M= Zr, Si, Ti) nanocomposite membranes for higher temperature PEM fuel cells. *Electrochim. Acta* **2005**, *51*, 553–560. [CrossRef]
75. Pan, J.; Zhang, H.; Chen, W.; Pan, M. Nafion–zirconia nanocomposite membranes formed via in situ sol–gel process. *Int. J. Hydrog. Energy* **2010**, *35*, 2796–2801. [CrossRef]
76. Koók, L.; Bakonyi, P.; Harnisch, F.; Kretzschmar, J.; Chae, K.-J.; Zhen, G.; Kumar, G.; Rózsenberszki, T.; Tóth, G.; Nemestothy, N.; et al. Biofouling of membranes in microbial electrochemical technologies: Causes, characterization methods and mitigation strategies. *Bioresour. Technol.* **2019**, *279*, 327–338. [CrossRef]
77. Handok, C.T.; Huda, A.; Gulo, F. Synthesis Pathway and Powerful Antimicrobial Properties of Silver Nanoparticle: A Critical Review. *Asian J. Sci. Res.* **2019**, *12*, 1–17. [CrossRef]
78. Basri, H.; Ismail, A.; Aziz, M. Polyethersulfone (PES)–silver composite UF membrane: Effect of silver loading and PVP molecular weight on membrane morphology and antibacterial activity. *Desalination* **2011**, *273*, 72–80. [CrossRef]
79. Liu, X.; Foo, L.-X.; Li, Y.; Lee, J.-Y.; Cao, B.; Tang, C.Y. Fabrication and characterization of nanocomposite pressure retarded osmosis (PRO) membranes with excellent anti-biofouling property and enhanced water permeability. *Desalination* **2016**, *389*, 137–148. [CrossRef]
80. Davies, R.L.; Etris, S.F. The development and functions of silver in water purification and disease control. *Catal. Today* **1997**, *36*, 107–114. [CrossRef]
81. Trevors, J. Silver resistance and accumulation in bacteria. *Enzym. Microb. Technol.* **1987**, *9*, 331–333. [CrossRef]
82. Feng, Q.L.; Wu, J.; Chen, G.Q.; Cui, F.Z.; Kim, T.N.; Kim, J.O. A mechanistic study of the antibacterial effect of silver ions on Esche-richia coli and Staphylococcus aureus. *J. Biomed. Mater. Res.* **2000**, *52*, 662–668. [CrossRef]
83. Coleman, M.; Koros, W. Isomeric polyimides based on fluorinated dianhydrides and diamines for gas separation applications. *J. Membr. Sci.* **1990**, *50*, 285–297. [CrossRef]
84. Hess, S.; Staudt-Bickel, C.; Lichtenthaler, R. Propene/propane separation with copolyimide membranes containing silver ions. *J. Membr. Sci.* **2006**, *275*, 52–60. [CrossRef]

85. Ahamed, M.; Karns, M.; Goodson, M.; Rowe, J.; Hussain, S.M.; Schlager, J.J.; Hong, Y. DNA damage response to different surface chemistry of silver nanoparticles in mammalian cells. *Toxicol. Appl. Pharmacol.* **2008**, *233*, 404–410. [CrossRef] [PubMed]

86. Robeson, L.M. Correlation of separation factor versus permeability for polymeric membranes. *J. Membr. Sci.* **1991**, *62*, 165–185. [CrossRef]

87. Hosseini, S.S.; Li, Y.; Chung, T.-S.; Liu, Y. Enhanced gas separation performance of nanocomposite membranes using MgO nanoparticles. *J. Membr. Sci.* **2007**, *302*, 207–217. [CrossRef]

88. Borkow, G.; Gabbay, J. Copper, An Ancient Remedy Returning to Fight Microbial, Fungal and Viral Infections. *Curr. Chem. Biol.* **2009**, *3*, 272–278. [CrossRef]

89. Ingle, A.P.; Durán, N.; Rai, M. Bioactivity, mechanism of action, and cytotoxicity of copper-based nanoparticles: A review. *Appl. Microbiol. Biotechnol.* **2014**, *98*, 1001–1009. [CrossRef]

90. Kanninen, P.; Johans, C.; Merta, J.; Kontturi, K. Influence of ligand structure on the stability and oxidation of copper nanoparticles. *J. Colloid Interface Sci.* **2008**, *318*, 88–95. [CrossRef]

91. Bassyouni, M.; Abdel-Aziz, M.; Zoromba, M.S.; Abdel-Hamid, S.; Drioli, E. A review of polymeric nanocomposite membranes for water purification. *J. Ind. Eng. Chem.* **2019**, *73*, 19–46. [CrossRef]

92. Palza, H.; Quijada, R.; Delgado, K. Antimicrobial polymer composites with copper micro- and nanoparticles: Effect of particle size and polymer matrix. *J. Bioact. Compat. Polym.* **2015**, *30*, 366–380. [CrossRef]

93. Ben-Sasson, M.; Zodrow, K.; Genggeng, Q.; Kang, Y.; Giannelis, E.P.; Elimelech, M. Surface Functionalization of Thin-Film Composite Membranes with Copper Nanoparticles for Antimicrobial Surface Properties. *Environ. Sci. Technol.* **2014**, *48*, 384–393. [CrossRef] [PubMed]

94. Ma, W.; Soroush, A.; Luong, T.V.A.; Brennan, G.; Rahaman, S.; Asadishad, B.; Tufenkji, N. Spray- and spin-assisted layer-by-layer assembly of copper nanoparticles on thin-film composite reverse osmosis membrane for biofouling mitigation. *Water Res.* **2016**, *99*, 188–199. [CrossRef]

95. Zhu, J.; Wang, J.; Uliana, A.A.; Tian, M.; Zhang, Y.; Zhang, Y.; Volodin, A.; Simoens, K.; Yuan, S.; Li, J.; et al. Mussel-Inspired Architecture of High-Flux Loose Nanofiltration Membrane Functionalized with Antibacterial Reduced Graphene Oxide–Copper Nanocomposites. *ACS Appl. Mater. Interfaces* **2017**, *9*, 28990–29001. [CrossRef]

96. Chen, S.; Zheng, J.; Li, L.; Jiang, S. Strong Resistance of Phosphorylcholine Self-Assembled Monolayers to Protein Adsorption: Insights into Nonfouling Properties of Zwitterionic Materials. *J. Am. Chem. Soc.* **2005**, *127*, 14473–14478. [CrossRef]

97. Zhang, R.; Liu, Y.; He, M.; Su, Y.; Zhao, X.; Elimelech, M.; Jiang, Z. Antifouling membranes for sustainable water purification: Strategies and mechanisms. *Chem. Soc. Rev.* **2016**, *45*, 5888–5924. [CrossRef]

98. Chen, S.; Li, L.; Zhao, C.; Zheng, J. Surface hydration: Principles and applications toward low-fouling/nonfouling biomaterials. *Polym.* **2010**, *51*, 5283–5293. [CrossRef]

99. Chang, Y.; Shih, Y.-J.; Lai, C.-J.; Kung, H.-H.; Jiang, S. Blood-Inert Surfaces via Ion-Pair Anchoring of Zwitterionic Copolymer Brushes in Human Whole Blood. *Adv. Funct. Mater.* **2013**, *23*, 1100–1110. [CrossRef]

100. Huang, C.-J.; Brault, N.D.; Li, Y.; Yu, Q.; Jiang, S. Controlled Hierarchical Architecture in Surface-initiated Zwitterionic Polymer Brushes with Structurally Regulated Functionalities. *Adv. Mater.* **2012**, *24*, 1834–1837. [CrossRef]

101. Shaoyi, J.; Jiang, S. Molecular Understanding and Design of Zwitterionic Materials. *Adv. Mater.* **2015**, *27*, 15–26. [CrossRef]

102. Choi, H.; Jung, Y.; Han, S.; Tak, T.; Kwon, Y.-N. Surface modification of SWRO membranes using hydroxyl poly(oxyethylene) methacrylate and zwitterionic carboxylated polyethyleneimine. *J. Membr. Sci.* **2015**, *486*, 97–105. [CrossRef]

103. Liu, F.; Ma, B.-R.; Zhou, D.; Xiang, Y.-H.; Xue, L.-X. Breaking through tradeoff of Polysulfone ultrafiltration membranes by zeolite 4A. *Microporous Mesoporous Mater.* **2014**, *186*, 113–120. [CrossRef]

104. Han, R.; Zhang, S.; Liu, C.; Wang, Y.; Jian, X. Effect of NaA zeolite particle addition on poly(phthalazinone ether sulfone ketone) composite ultrafiltration (UF) membrane performance. *J. Membr. Sci.* **2009**, *345*, 5–12. [CrossRef]

105. He, T.; Zhou, W.; Bahi, A.; Yang, H.; Ko, F. High permeability of ultrafiltration membranes based on electrospun PVDF modified by nanosized zeolite hybrid membrane scaffolds under low pressure. *Chem. Eng. J.* **2014**, *252*, 327–336. [CrossRef]

106. Leo, C.; Kamil, N.A.; Junaidi, M.; Kamal, S.; Ahmad, A.L. The potential of SAPO-44 zeolite filler in fouling mitigation of polysulfone ultrafiltration membrane. *Sep. Purif. Technol.* **2013**, *103*, 84–91. [CrossRef]

107. Wee, S.-L.; Tye, C.-T.; Bhatia, S. Membrane separation process—Pervaporation through zeolite membrane. *Sep. Purif. Technol.* **2008**, *63*, 500–516. [CrossRef]

108. Kunnakorn, D.; Rirksomboon, T.; Aungkavattana, P.; Kuanchertchoo, N.; Atong, D.; Kulprathipanja, S.; Wongkasemjit, S. Performance of sodium A zeolite membranes synthesized via microwave and autoclave techniques for water–ethanol separation: Recycle-continuous pervaporation process. *Desalination* **2011**, *269*, 78–83. [CrossRef]